Elobixibat, an Ileal Bile Acid Transporter Inhibitor, Ameliorates Non-alcoholic Steatohepatitis in Mice

Ryo Yamauchi[1], Hidetoshi Takedatsu[1], Keiji Yokoyama[1], Eri Yamauchi[1], Motoko Kawashima[1], Takahiro Nagata[1], Yotaro Uchida[1], Takanori Kitaguchi[1], Tomotaka Higashi[1], Hiromi Fukuda[1], Naoaki Tsuchiya[1], Kazuhide Takata[1], Takashi Tanaka[1], Daisuke Morihara[1], Yasuaki Takeyama[1], Satoshi Shakado[1], Shotaro Sakisaka[2], and Fumihito Hirai[1]

1) Department of Gastroenterology and Medicine, Fukuoka University Faculty of Medicine, Fukuoka, Japan

2) The Center of Medical Science, Fukuoka University Faculty of Medicine, Fukuoka, Japan

***Corresponding author:** Dr. Hidetoshi Takedatsu

Department of Gastroenterology and Medicine, Fukuoka University Faculty of Medicine, 7-45-1 Nanakuma, Jonan-ku, Fukuoka, Fukuoka 814-0180, Japan.

TEL: +81-92-801-1011 Ext: 3355; Fax: +81-92-874-2663

E-Mail: htakedatsu@gmail.com

Authors' email addresses

Ryo Yamauchi: r_christinue2017@yahoo.co.jp

Hidetoshi Takedatsu: htakedatsu@gmail.com

Keiji Yokoyama: yokotin@fukuoka-u.ac.jp

Eri Yamauchi: eyamauchi@fukuoka-u.ac.jp

Motoko Kawashima: motoko@fukuoka-u.ac.jp

Takahiro Nagata: takahiro1328@hotmail.co.jp

Yotaro Uchida: yoota86@gmail.com

Takanori Kitaguchi: kitaguchitakanori@gmail.com

Tomotaka Higashi: kolsehvahn666@gmail.com

Hiromi Fukuda: hiromi.m.0928@gmail.com

Naoaki Tsuchiya: tottydesuyo@gmail.com

Kazuhide Takata: edihuzak_t@yahoo.co.jp

Takashi Tanaka: tanaka329@yahoo.co.jp

Daisuke Morihara: morihara@fukuoka-u.ac.jp

Yasuaki Takeyama: yaz@fukuoka-u.ac.jp

Satoshi Shakado: shakado@cis.fukuoka-u.ac.jp

Shotaro Sakisaka: sakisaka@fukuoka-u.ac.jp

Fumihito Hirai: fuhirai@cis.fukuoka-u.ac.jp

Acknowledgements

We thank Mark Cleasby, PhD, from Edanz Group (https://en-author-services.edanzgroup.com/ac) for editing a draft of this manuscript.

Elobixibat, an Ileal Bile Acid Transporter Inhibitor, Ameliorates Non-alcoholic Steatohepatitis in Mice

Abstract

Background: Recent studies have suggested that several types of toxic bile acids (BAs) are involved in the pathogenesis of non-alcoholic steatohepatitis (NASH). In the present study we aimed to determine whether elobixibat, an ileal bile acid transporter (IBAT) inhibitor, would ameliorate NASH in mice.

Methods: C57BL/6N mice were fed a methionine and choline-deficient (MCD) or standard diet for 8 weeks (n=5 per group) to induce NASH. In addition, half of the MCD diet-fed mice were administered elobixibat 5 days a week for 4 weeks by gavage. The effects of the treatments on liver histopathology, proinflammatory cytokine concentrations, intestinal epithelial tight junctions, and the intestinal microbial composition were then assessed.

Results: In MCD-fed mice, hepatic fibrosis and inflammatory cell infiltration developed, and the serum aspartate transaminase activity and BA concentration were higher than the control. In addition, the proinflammatory cytokine concentrations were high in the liver and mesenteric lymph nodes (MLN), and the expression of intestinal epithelium tight junction proteins, claudin1, was increased. In the intestinal microbial composition, the abundance of the Lachnospiraceae and Ruminococcaeae were decreased, whereas that of the Enterobacteriaceae was increased. Treatment with elobixibat

reduced the serum and increased the fecal BA concentration, and ameliorated the liver inflammation and fibrosis. It also reduced the expression of proinflammatory cytokines in the liver and MLNs, and transforming growth factor-β expression in the liver. Finally, elobixibat normalized intestinal tight junction protein level and the composition of the intestinal microbiota.

Conclusion: Elobixibat ameliorates NASH-related histopathology, reduces cytokine expression, and normalizes the intestinal microbial composition in MCD-fed mice, which suggests that it may represent a promising candidate for the therapy of NASH.

Keywords: Non-alcoholic steatohepatitis; Steatosis; Liver fibrosis; Liver inflammation; Treatment; Elobixibat; Ileal bile acid transporter; Bile acid; Gut microbiota; Mesenteric lymph node

Abbreviations

NAFLD, non-alcoholic fatty liver disease; NASH, non-alcoholic steatohepatitis; BAs, bile acids; IBAT, ileal bile acid transporter; HFD, high-fat diet; LDL, low-density lipoprotein; TJ, tight junction; MCD, methionine and choline-deficient; AST, aspartate transaminase; HE, hematoxylin and eosin; NAS, NAFLD activity score; TBS, tris-buffered saline; MLN, mesenteric lymph node; TNF-α, tumor necrosis factor-α; IL-6, interleukin-6; TGF-β, transforming growth factor-β; RT, room temperature; RDP, ribosomal database project; HCC, hepatocellular carcinoma; HSCs, hepatic stellate cells; ROS, reactive oxygen species.

Introduction

Non-alcoholic fatty liver disease (NAFLD) is closely associated with features of the metabolic syndrome, such as central obesity, insulin resistance, and dyslipidemia.[1] Because of the increase in the prevalence of obesity, the prevalence of NAFLD has increased by 20%–30% in recent years.[2,3] NAFLD comprises a range of histopathological grades from mild steatosis to severe non-alcoholic steatohepatitis (NASH),[2] and about 10% of NAFLD patients progress to NASH, which is characterized by intrahepatic fat of at least 5% of the total liver weight, inflammation and hepatocyte ballooning.[3] Furthermore, hepatocellular carcinoma (HCC) was developed in patients with NASH and the incident rate has been estimated to be 2.6%–12.8%.[4] The progression to NASH is a complex and multifactorial process that involves genetic and environmental factors.

Bile acids (BAs) are synthesized from cholesterol in the liver and secreted as the major component of bile. Ninety-five percent of BAs are reabsorbed in the ileum *via* the ileal bile acid transporter (IBAT) and delivered to the liver by the portal vein.[5] BAs regulate cholesterol homeostasis, lipid solubilization, and metabolic signaling in the liver.[6] A previous study showed that the histological severity of NASH correlates with the serum BA concentration,[6] and it has also been shown that a high serum BA concentration increases the risk of hepatotoxicity, owing to activation of inflammatory, oxidative stress, and necrotic cell death pathways in patients with NAFLD or NASH.[7] Therefore, there is evidence that high serum BA concentration is involved in the pathogenesis of NASH.

Several previous studies have shown that the inhibition of IBAT ameliorates hepatic inflammation and fibrosis.[8-10] Administration of the IBAT inhibitor SC-435 reduces serum cholesterol in high-fat diet (HFD)-induced fatty liver disease[9] and ameliorates atherosclerosis and NAFLD in several rodent models.[10, 11] In 2018, elobixibat (formerly A3309), another IBAT inhibitor, was approved as a treatment for chronic idiopathic constipation in Japan. It prevents the reabsorption of conjugated BAs in the ileum, which disrupts the enterohepatic circulation and increases the fecal loss of BAs. The increase in colonic BA concentration promotes the secretion of water and electrolytes into the colonic lumen and increases intestinal motility. Furthermore, elobixibat has been reported to reduce serum low-density lipoprotein (LDL)-cholesterol concentrations in both animal studies and clinical trials.[12]

Changes in the composition of the intestinal microbiota is also thought to be involved in the progression of NASH, because previous studies have shown that improvements in this microbiota composition reduce inflammation in liver. A sub-analysis of the composition of the microbiota showed that the abundance of Ruminococcus and Faecalibacterium was associated with the progression of NASH.[13] Furthermore, intestinal permeability is high in patients with NAFLD,[14] because of disruption of intestinal epithelial tight-junctions (TJs), and correlates with the severity of hepatic inflammation. In murine models of NAFLD, gut bacterial overgrowth and compositional changes increase intestinal permeability by reducing the expression of TJ proteins.[14]

In the present study, we aimed to determine the effects of elobixibat in a mouse model of

NASH, including its effects on the liver, the intestinal microbiota, and intestinal TJs.

Material and Methods

Animal model and experimental design

Male 5-to 6-week-old C57BL/6N mice were purchased from SLC (Fukuoka, Japan) and were housed under specific pathogen-free conditions at Fukuoka University. All the animal procedures were performed in accordance with the ethical standards of the institution and ethics approval was obtained from The Animal Care and Use Committee of Fukuoka University (Permit number: 2090). The mice were acclimatized to their surroundings for 1 week, while consuming a standard diet, after which they were randomly allocated to three groups. One group was fed a standard diet (CRF-1, Oriental Yeast Co., ltd., Tokyo, Japan) for 8 weeks (control group); a second group was fed a methionine and choline-deficient (MCD) diet (A02082002B, Research Diets Inc., New Brunswick, NJ, USA) for 8 weeks (the NASH group); and the third was fed the MCD diet fed for 8 weeks, and elobixibat (1.2 mg/kg/day, EA Pharma., Tokyo, Japan) was administered for the final 4 weeks of this period (elobixibat group). At the end of the study period, the mice were euthanized by inhalation of carbon dioxide.

Administration of elobixibat

Doses of 0.2, 0.6, or 1.2 mg/kg of elobixibat were administered for 4 weeks, 5 days per

week, by oral gavage. Both the control group and the MCD-NASH group were administered PBS on the same schedule by oral gavage. There were no clear effects of 0.2 mg/kg or 0.6 mg/kg (data not shown), but beneficial effects were observed at the 1.2 mg/kg/day dose. This concentration is 4-6 times the dosage for human. According to “Drug Interview Form of Elobixibat”, elobixibat showed strong inhibitory activity to human IBAT, which was about four times more than it to mouse IBAT. Therefore, a dose of 1.2 mg/kg/day in mice is considered equivalent to 0.3 mg/kg/day in human. We evaluated the effects of this dose on the severity of NASH, cytokine production, the intestinal microbiota, and the intestinal TJs in the mice. No diarrhea was observed during the rearing period, and there was no difference in body weight between the NASH and elobixibat groups at the end of the experiment.

Blood and fecal sampling and analysis

After 8 weeks, the mice were sacrificed, and blood samples were obtained by cardiac puncture. The blood samples were centrifuged, and serum was collected for the measurement of serum aspartate transaminase (AST) activity and BA concentration. Total fecal BA content was measured using a Total bile acid assay kit (Cell Biolabs, Inc., San Diego, USA).

Isolation of mesenteric lymph nodes

Euthanize the mouse using carbon dioxide narcosis, made a midline incision with scissors,

and expose the peritoneal cavity. Locate the caecum and gently pull the caecum down with forceps. Use forceps to carefully move the small intestine to the right, exposing the entire mesenteric lymph nodes (MLNs) chain, which is aligned the colon and identify the bottom node in the chain, located closest to the cecum. Use one set of forceps to grasp the mesentery/fat around it and gently remove the MLN chain from the bottom to the top.[15]

Histological analysis and immunohistochemical staining

After sacrifice, portions of the liver of each mouse were fixed in 10% formalin for sectioning and hematoxylin and eosin (HE) and Sirius red staining. The sections were evaluated histopathologically using the NAFLD activity score (NAS).[3] The NAS grades the severity of NASH on the basis of scores for steatosis, inflammation, and ballooning, and a score of $\geq$5 points out of 8 defines NASH. The fibrosis scores were as follows: 1, mild pericellular and perivenular fibrosis; 2, moderate pericellular and perivenular fibrosis; 3, bridging fibrosis with lobular distortion; and 4, cirrhosis.

The ileum of each mouse was washed with PBS buffer and fixed in 10% formalin. Tissue sections were then prepared and subjected to immunostaining. The endogenous peroxidase activity was blocked using H_2O_2 in Tris-buffered saline (TBS), then the sections were incubated overnight in a 1:200 dilution of rabbit polyclonal anti-mouse claudin-1 (CLDN1) antibody (Santa Cruz, Biotechnology, Dallas, TX). The liver sections were observed and analyzed using the All-in-one

Fluorescence Microscope BZ-X710 (KEYENCE Corporation, Osaka, Japan). For immunohistochemistry, the tissue sections were examined under the AxioVision Imaging software (version 4.8; Carl Zeiss, Gottingen, Germany).

Real-time PCR

RNA was extracted from the liver, ileum, and MLNs of the mice using TRIzol (Invitrogen, Carlsbad, CA, USA) and concentration with 260/280 quality ratio for all isolated RNA samples were determined using the Nanodrop spectrophotometer (Wilmington, DE, USA). The RNA was reverse transcribed into cDNA with SuperScript™ IV VILO™ Master Mix (Invitrogen, Carlsbad, CA, USA). The cDNA was quantified using real-time PCR (RT-PCR) with TaqMan Fast Universal PCR Master Mix (2x) in the Applied Biosystems Inc., (ABI) StepOnePlus Real-Time PCR instrument (ABI, CA, USA). These probes are marketed from TaqMan (ABI). Liver cDNA was subjected to RT-PCR to measure the expression of tumor necrosis factor-α (*Tnf*) mRNA, interleukin-6 (*Il6*) mRNA, and transforming growth factor-β (*Tgif1*) mRNA, and ileal cDNA was subjected to RT-PCR to measure the expression of *Cldn1* mRNA. MLN samples were also subjected to RT-PCR to measure the expression of *Tnf* and *Il6* mRNA. The expression of each mRNA is expressed relative to that of the reference gene *Gapdh*. The primers used were as follows: *Cldn1*: Mm00516701_m1, *Cldn3*: Mm00515499_s1, *Tnf*: Mm99999068_m1, *Il6*: Mm00446190_m1, *Tgif1*: Mm01227699_m1, and *Gapdh*: Mm99999915_g1. The results were quantified using the $2^{-\Delta\Delta CT}$ method and are expressed as

a fold difference from the control group. The *Gapdh* gene was chosen as the reference gene because of its uniform expression throughout the samples evaluated.

Western blotting

Samples of colon and ileum were lysed in Complete Lysis-M reagent (Roche, Mannheim, Germany) containing protease and phosphatase inhibitors, according to the manufacturer's instructions. Lysates containing equal amounts of protein were then separated by SDS-PAGE and transferred to methanol-activated PVDF membranes (Millipore, Beijing, China). The membranes were blocked with PVDF Blocking Reagent (Toyobo, Tokyo, Japan) at room temperature (RT) for 1 h, and then incubated with primary antibody at RT for 1 h, washed, and incubated with secondary HRP-conjugated sheep anti-mouse IgG antibody (GE Healthcare, Buchinghamshire, UK). Western blot analysis was performed according to standard procedures using ECL Prime Western Blotting Detection Reagents (GE Healthcare, Amersham, UK). Image capture and analysis were performed using an ImageQuant LAS 3000 system (Fujifilm, Tokyo, Japan). The protein expression of the target protein was normalized to that of β-actin. Anti-CLDN1 (sc-81796) antibody was from Santa Cruz Biotechnology, Inc (Heidelberg, Germany) and anti-β-actin (A1978) antibody was from Sigma-Aldrich (St. Louis, MO, USA). Densitometric analysis of the Western blots was undertaken using ImageJ as described previously [16].

Analysis of the intestinal microbial composition

Fecal samples were collected from the mice at the end of the study period, immediately frozen, and stored at <−20°C until analysis. DNA extraction and cluster analysis were performed using terminal restriction fragment length polymorphism analysis at TechnoSuruga Laboratory Co., Ltd. (Shizuoka, Japan).

Frozen fecal samples were thawed on ice, 100 mg of each sample was suspended in 4 M guanidium thiocyanate, 100 mM Tris-HCl (pH 9.0), and 40 mM EDTA, and the samples were then beaten with zirconia beads using a FastPrep FP100A instrument (MP Biomedicals, USA). DNA was extracted from the resulting suspensions using a Magtration System 12GC and GC series MagDEA DNA 200 (Precision System Science, Japan). The concentrations of DNA in each extract were measured by spectrophotometry using an ND-1000 instrument (NanoDrop Technologies, USA), and the final concentration of each was adjusted to 10 ng/μL. The DNA was then further extracted using an automated DNA isolation system (Gene Prep Star PI-480; Kurabo, Japan). The V3–V4 regions of the bacterial 16S rRNA genes were amplified using 341F/806R primers and the dual-index method. Bar-coded amplicons were paired-end sequenced using 2×284-bp cycles on a MiSeq system with MiSeq Reagent Kit version 3 (600 Cycle) chemistry.

The paired-end sequencing reads were merged using the Fastq-join program, with default settings. Only joined reads that had quality scores of ≥ 20 for more than 99% of a sequence were extracted using FASTX-Toolkit. Chimeric sequences were deleted using Usearch6.1. The

identification of bacterial taxa from the analyses of sequence reads was performed manually using the Ribosomal Database Project (RDP) Multiclassifier tool (http://rdp.cme.msu.edu/classifier/). Bacterial species were also identified from the sequences using Metagenome@KIN Ver 2.2.1 analysis software (World Fusion, Japan) and the TechnoSuruga Lab Microbial Identification database DB-BA 13.0, with an accepted homology level of ≥ 97%.

Statistical analysis

All the data are presented as the mean ± standard deviation (SD). Statistical analyses were performed using t-test and ANOVA for blood test results, PCR and fat droplets count, and statistical evaluation of Score was performed by Mann-Whitney U test and Kruskal-Mallis test. JMP software version 13 was used for this evaluation. $p < 0.05$ was considered to represent statistical significance.

Results

Consumption of an MCD diet induces hepatic fibrosis and inflammatory cell infiltration

Eight weeks of consumption of an MCD diet induced NASH in the mice. Examination of liver sections revealed advanced fibrosis, inflammatory cell infiltration, and steatosis in the NASH group, but not in the control group (Figure 1A). Both the serum AST activity and BA concentration were significantly higher in the NASH group than in the control group ($p < 0.01$, Figure 1B, 1C). The hepatic mRNA expression of TNF-α, IL-6, and TGF-β, which promotes liver fibrosis, were also

significantly higher in the NASH group than the control group ($p < 0.01$, Figure 2A), as was the expression of TNF-α and IL-6 in MLNs ($p < 0.01$, Figure 2B).

Next, we measured the expression of the intestinal TJ protein claudin-1 and claudin-3 in the terminal ileum, to determine whether NASH is associated with changes in the intestinal epithelial barrier. We found that the mRNA expression of *Cldn1* and the level of claudin-1 protein in the terminal ileum were higher in the NASH group than in the control group ($p < 0.05$, Figure 3A, B). Additionally, the mRNA expression of *Cldn3* were lower in the NASH group than in the control group. (Supplementary figure 1) Immunohistochemical staining showed villial atrophy and high levels of claudin-1 protein in the intercellular spaces in the intestinal epithelium (Figure 3C). Therefore, the MCD diet not only induced NASH, but also affected the intestinal epithelium.

Elobixibat ameliorates the liver fibrosis and reduces the serum lipid and BA concentrations in mice with NASH

Elobixibat tended to reduce serum AST activity, but this effect did not achieve significance (elobixibat group: 629.6±51 U/L *vs*. NASH group: 706.2±51 U/L, $p = 0.3189$). HE and Sirius red staining of liver sections showed the presence of an inflammatory cell infiltrate, steatosis, and fibrosis in the NASH group (Figure 4A), but the fibrosis was mild and there were few inflammatory cells in the elobixibat group (Figure 4A), such that the NAS and fibrosis score were significantly lower in the elobixibat group (Figure 4B). The serum BA concentration was also significantly lower

in the elobixibat group than in the NASH group ($p < 0.01$, Figure 4C), whereas the fecal BA content was higher ($p < 0.01$, Figure 4D).

Elobixibat reduces proinflammatory cytokine and TGF-β-mRNA expression in mice with NASH

To investigate the mechanism by which elobixibat ameliorates hepatic inflammation in mice with NASH, we measured the mRNA expression of TNF-α and IL-6 in the liver, and found that the expression of both was significantly lower in the elobixibat group than in the NASH group (Figure 5A). Moreover, to determine the mechanism by which elobixibat suppresses hepatic fibrosis in mice with NASH, we measured the expression of TGF-β, the principal regulator of fibrosis in the liver, and found that the administration of elobixibat reduces the hepatic expression of TGF-β (Figure 5B). Interestingly, the administration of elobixibat also reduced the expression of TNF-α and IL-6 in MLNs (Figure 5C).

Elobixibat reduces intestinal claudin-1 expression in mice with NASH

Intestinal permeability is controlled by TJ proteins. The expression of *Cldn1* mRNA was significantly lower in the elobixibat group than in the NASH group ($p < 0.05$, Figure 6A), as was the claudin-1 protein level in the intestinal mucosa (Figure 6B, C). However, there was no difference in the expression of *Cldn3* mRNA between elobixibat group and the NASH group (Supplementary figure 1).

Next, we determined the effect of elobixibat on the intestinal microbial composition, and found that the consumption of an MCD diet reduced the abundance of the Lachnospiraceae and Ruminococcaeae, and increased the abundance of the Enterobacteriaceae in the feces of the mice, compared with the control group. In contrast, the abundance of the Lachnospiraceae and Ruminococcaeae increased and that of the Enterobacteriacease was reduced by elobixibat administration (Figure 6D).

Discussion

The results of the present study demonstrate that the administration of elobixibat to mice with NASH ameliorates inflammation and fibrosis in the liver and improves the composition of the intestinal microbiota. These effects may reflect the effects of the drug on serum and fecal BA concentrations.

Recently, the accumulation of BAs has been shown to play a major role in liver injury in chronic liver diseases,[17] and high serum concentrations have been reported in patients with obesity and metabolic syndrome-related diseases, such as type 2 diabetes mellitus and NAFLD/NASH[18, 12]. Furthermore, several studies have shown that serum BA concentrations are high in patients and rodents with cirrhotic NASH, whereas the fecal concentrations are low.[7,19-20] Sydor et al. reported that serum BA were 2-3 times higher in NASH compared with healthy controls. Furthermore, serum BAs in cirrhotic NASH were significantly increased 10 times more compared to

healthy controls as the MCD model mice.[21] In the present study, the serum BA concentration was significantly increased and that of fecal BA was reduced by the consumption of an MCD diet. Because previous studies have demonstrated that high serum BA concentrations are involved in the progression of NASH, we hypothesized that this reduction in serum BA concentration would ameliorate NASH, and indeed, we found that elobixibat also ameliorated liver inflammation and fibrosis in the mice.

Hepatic stellate cells (HSCs) are important mediators of liver fibrosis.[22] In hepatocytes, BAs induce the formation of reactive oxygen species (ROS), which induce the activation of HSCs. In addition, BAs activate nuclear factor κB in HSCs *via* the TNFα signaling pathway, and HSCs produce IL-6 and TGF-β in response to liver injury.[22] In the present study, the high hepatic TNF-α, IL-6, and TGF-β mRNA expression that was induced by MCD consumption was ameliorated by elobixibat. This is consistent with TNF-α, IL-6, and TGF-β production by HSCs being stimulated by the high BA concentration, and the increase in expression being ameliorated by elobixibat, thereby ameliorating the liver inflammation and fibrosis.

TJs form an intestinal barrier that protects the host against intestinal bacteria and their products. In the present study, the MCD diet induced not only NASH, but also inflammation in MLNs and an increase in the expression of claudin-1. Previous studies have also shown that claudin-1 expression is upregulated during active intestinal inflammation.[23, 24] Furthermore, the secretion of TNF-α and bacterially-derived endotoxin induce increases in intestinal TJ protein

expression, and especially that of claudin-1.[23-27] The high expression of claudin-1 may protect the intestinal epithelium against the local inflammation and damage that is induced alongside NASH. However, we found that the intestinal expression of claudin-1 and the hepatic and MLN expression of TNF-α and IL-6 was significantly reduced by the administration of elobixibat.

An association between gut dysbiosis and NASH has been demonstrated using mouse models of gut microbial transplantation.[28] Transfer of bacteria or bacterial products into the portal circulation is a major mechanism whereby gut dysbiosis may be linked with the progression of chronic liver diseases. In the present study, intestinal microbiome analysis showed that the abundance of the Lachnospiraceae and Ruminococcaeae were decreased, whereas that of the Enterobacteriaceae was increased in mice with NASH compare to control mice. The administration of elobixibat restored the intestinal microbiota to their normal state. The family Lachnospiraceae is an important source of butyrate, which has been shown to inhibit intestinal inflammation, maintain the intestinal barrier, and modulate gut motility.[29] The family Ruminococcaceae, which is belongs to the genus Clostridium and produces butyric acid, is a source of energy for the epithelial cells of the intestine. As we have shown in MCD model mice, Kim et al. demonstrated that the family Lachnospiraceae and the family Ruminococcaceae in the NAFLD patients were significantly lower than healthy patients.[30] Therefore, the increase in the genera Lachnospiraceae and Ruminococcaeae by elobixibat might contribute to the improvement of NASH in mice model. In addition, the family Enterobacteriaceae, including symbionts Escherichia coli and Proteus spp., are a

large family of gram-negative facultative bacteria. Enterobacteriaceae are among the most commonly overgrown symbionts in many conditions such as inflammatory bowel disease, obesity, and antibiotic treatment.[31] The reduction of Enterobacteriaceae by elobixibat also might contribute the decrease of proinflammatory cytokines.

Recent study showed that the benefit of elobixibat in chronic constipation was associated with the increase of fecal deoxycholic acid (DCA), but not effects of altered microbiota.[32] In NASH patients, there was no significant difference of fecal BA between healthy control and NASH, although serum BA was elevated in NASH patients. However, the alteration of intestinal microbiota was observed.[33] In the present study, the administration of elobixibat did not directly affect stool properties, however fecal BA was significantly increased. Therefore, we supposed that elobixibat was increased the fecal BA, which has the most potent antimicrobial activity in the colon [34] and caused normalization of the intestinal microbiota.

An IBAT inhibitor has already been shown to increase the fecal content of primary BAs and to reduce the serum concentration of these highly toxic substances.[35] Therefore, the increase in the content of primary BAs induced by the administration of elobixibat might be responsible for the amelioration of the gut dysbiosis associated with NASH. The limitation of our study is the use of MCD diet-induced NASH model. MCD model mice have decreased serum triglyceride, cholesterol, insulin, leptin and weight loss, on the other hand the character of NASH in human have reported high saturated fat and cholesterol ingestion leading to weight gain, elevated serum triglyceride and

cholesterol. Furthermore, the factor for steatosis in MCD is defective hepatic lipid export/VLDL synthesis and elevated beta-oxidation, whereas the factor for steatosis in human NASH is elevated fatty acids esterification versus beta-oxidation driven by lipid overload. [36] Furthermore, the factor for steatosis in MCD is defective hepatic lipid export/VLDL synthesis and elevated beta-oxidation, whereas the factor for steatosis in human NASH is elevated fatty acids esterification versus beta-oxidation driven by lipid overload.

In summary, we have shown that the administration of elobixibat to mice with NASH ameliorates their high serum BA concentration and gut dysbiosis, which may be responsible for the reduction in expression of TNF-α and IL-6 in the liver and MLNs, and a consequent amelioration of NASH. These findings suggest that elobixibat might have potential as a treatment for NASH.

Funding

This research did not receive any specific grant from funding agencies in the public, commercial, or not–for–profit sectors.

Ethical Requirements

All procedures performed in studies involving animals were in accordance with the ethical standards of the institution at which the studies were conducted and ethical approval was obtained

from The Animal Care and Use Committee of Fukuoka University (Permit number: 2090). This article does not contain any studies with human participants performed by any of the authors.

Conflict of interest

All the authors declare that they have no conflict of interest.

References

[1] Dowman JK, Tomlinson JW, Newsome PN. Pathogenesis of non-alcoholic fatty liver disease. QJM: Monthly Journal of the Association of Physicians. 2010; 103:71–83.

[2] Diehl, A.M., Day, C. Cause, Pathogenesis, and Treatment of Nonalcoholic Steatohepatitis. N. Engl J. 2017; 377, 2063-2072.

[3] Suga T, Yamaguchi H, Ogura J, Shoji S, Maekawa M, Mano N. Altered bile acid composition and disposition in a mouse model of non-alcoholic steatohepatitis. Toxicol Appl Pharmacol. 2019; 379:114664.

[4] George C, Ronak P, Sandeep K, Sanjaya KS. Hepatocellular carcinoma in non-alcoholic steatohepatitis: Current knowledge and implications for management. World J Hepatol. 2017; 9:11, 533-543.

[5] Chiang JY. Bile Acid Metabolism and Signaling. Compr Physiol. 2013 July; 3(3): 1191–1212.

[6] Puri P, Daita K, Joyce A, Mirshahi F, Santhekadur PK, Cazanave S, et al. The presence and severity of nonalcoholic steatosis associated with specific changes I circulating bile acids. Hepatology 2018; 67:534-548.

[7] Kalhan SC, Guo L, Edmison J, Dasarathy S, McCllough AJ, Hanson RW, et al. Plasma metabolomic profile in nonalcoholic fatty liver disease. Metab Clin Exp. 2011; 60:404–413.

[8] Arab JP, Karpen SJ, Dawson PA, Arrese M, Trauner M. Bile acids and nonalcoholic fatty liver disease: Molecular insights and therapeutic perspectives. Hepatology. 2017 Jan;65(1):350-362.

[9] Meithke, AG, Zhang W, Simmons J, Taylor AE, Shi T, Shanmukhappa, SK, et al. Pharmacological inhibition of apical sodium dependent bile acid transporter changes bile composition and blocks progression of sclerosing cholangitis in multidrug resistance 2 knockout mice. Hepatology 2016; 63, 512-523.

[10] Rao A, Kosters A, Mells JE, Zhang W, Setchell KD, Amanso AM, et al. Inhibitor of ileal bile acid uptake protects against nonalcoholic fatty liver disease in high-fat diet fed mice. Sci Trasl Med. 2016; 8: 357ra122.

[11] Bhant BG, Rapp SR, Beaudty JA, Napawan N, Butteiger DN, Hall KA, et al. Inhibitition of ileal bile acid transport and reduced atherosclerosis in apoE-/- mice by SC435. Lipid Res 2003; 44, 1614-1621.

[12] Al-Dury S, Marschall HU. Ileal Bile Acid Transporter Inhibition for the Treatment of Chronic Constipation, Cholestatic Pruritus, and NASH. Front Pharmacol. 2018; Aug 21;9:931.

[13] Duarte SMB, Stefano JT, Oliveira CP. Microbiota and nonalcoholic fatty liver disease/nonalcoholic steatohepatitis (NAFLD/NASH). Ann Hepatol. 2019; 18: 416-421.

[14] Brun P, Castagliuolo I, Leo DV, Buda A, Pinzani M, Palu G, Martines D. Increased intestinal permeability in obese mice: new evidence in the pathogenesis of nonalcoholic steatohepatitis. Am J Physiol Gastrointest Liver Physiol 2007; 292:G518–525.

[15] Qiu Z, Sheridan BS. Isolating Lymphocytes from the Mouse Small Intestinal Immune System. J Vis Exp. 2018;(132):57281.

[16] Gallo-Oller G, Ordoñez R, Dotor J. A new background subtraction method for Western blot densitometry band quantification through image analysis software. Journal of Immunological Methods. 2018;457:1–5.

[17] Fickert P, Wagner M. Biliary bile acids in hepatobiliary injury - What is the link? J. Hepatol. 2017; 67 619–631.

[18] Molinaro A, Wahlstrom A, Marschall HU. Role of bile acids in metabolic control. Trends Endocrinol. Metab. 2018; 29 31–41.

[19] Tanaka N, Matsubara T, Krausz KW, Patterson AD, Gonzalez FJ. Disruption of phospholipid and bile acid homeostasis in mice with nonalcoholic steatohepatitis. Hepatology. 2012; 56:118–129.

[20] Yamada S, Takashima Y, Watanabe M, Nagamine R, Saito Y, Kamada N, Saito H. Bile acid metabolism regulated by the gut microbiota promotes non-alcoholic steatohepatitis-associated hepatocellular carcinoma in mice. Oncotarget. 2018; 11:9925-9939.

[21] Svenja Sydor, Jan Best, et al Altered Microbiota Diversity and Bile Acid Signaling in Cirrhotic and Noncirrhotic NASH-HCC. Clinical and Translational Gastroenterology 2020;11:e00131.

[22] Saga K, Iwashita Y, Hidano S, Aso Y, Isaka K, Kido Y, et al. Secondary Unconjugated Bile Acids Induce Hepatic Stellate Cell Activation. Int J Mol Sci. 2018; 19:3043.

[23] Weber CR., Raleigh DR, Su L, Shen L, Sullivan EA, Wang Y, Turner JR. Epithelial myosin light chain kinase activation induces mucosal interleukin-13 expression to alter tight junction ion selectivity. J. Biol. Chem. 2010; 285, 12037–12046.

[24] Weber CR, Nalle SC, Tretiakova M, Rubin DT, Tumer JR. Claudin-1 and claudin-2 expression is elevated in inflammatory bowel disease and may contribute to early neoplastic transformation. Lab Invest. 2008; 1110-20.

[25] Poritz LS, Harris III LR, Kelly AA, Koltun WA. Increase in the tight junction protein claudin-1 in intestinal inflammation. Dig Dis Sci. 2011; 56: 2802-2809.

[26] Han X, Fink MP, Yang R, Delude RL. Increased iNOS activity is essential for intestinal epithelial tight junction dysfunction in endotoxemic mice. Shock. 2004; 21:261-70.

[27] Garcia-Hernandez V, Quiros M, Nusrat A. Intestinal epithelial claudins: expression and regulation in homeostasis and inflammation. Ann. NY Acad. Sci. 2017; 1397:66-79.

[28] Turnbaugh PJ, Ley RE, Mahowald MA, Magrini V, Mardis ER, Gordon JI. An obesity-associated gut microbiome with increased capacity for energy harvest. Nature. 2006; 444, pp. 1027-1031.

[29] Liu H, Wang J, He T, Becker S, Zhang G, Li D, Ma X. Butyrate: A Double-Edged Sword for Health? Adv Nutr. 2018; 21-29.

[30] Kim H.N, Joo E.J, Cheong H.S, Kim Y, Kim H.L, Shin H, Chang Y, Ryu S. Gut Microbiota and Risk of Persistent Nonalcoholic Fatty Liver Disease J Clin Med. 2019 Jul 24;8(8):1089.

[31] MY Zeng, N Inohara, and G Nuñez. Mechanisms of inflammation-driven bacterial dysbiosis in the gut. Mucosal Immunol. 2017 Jan; 10(1): 18–26.

[32] Noboru Misawa, Takuma Higurashi, Tomohiro Takatsu. The benefit of elobixibat in chronic

constipation is associated with faecal deoxycholic acid but not effects of altered microbiota. Alimentary Pharmacology & Therapeutics 52(5), 821-828, 2020.

[33] Svenja Sydor, Jan Best. Altered Microbiota Diversity and Bile Acid Signaling in Cirrhotic and Noncirrhotic NASH-HCC Clin Transl Gastroenterol. 2020 Mar; 11(3): e00131.

[34] Islam KB, Fukiya S, Hagio M, Fujii N, Ishizuka S, Ooka T, Ogura Y, Hayashi T, Yokota A. Bile acid is a host factor that regulates the composition of the cecal microbiota in rats. Gastroenterology. 2011 Nov; 141(5):1773-81.

[35] Graffner H, Gillberg PG, Rikner L, Marschall HU. The ileal bile acid transporter inhibitor A4250 decreases serum bile acids by interrupting the enterohepatic circulation. Aliment Pharmacol Ther. 2016; Jan;43(2):303-10

[36] Donnelly KI, Smith CI, Schwarzenberg SJ, Jessurun J, Boldt MD, Parks EJ. Sources of fatty acids stored in liver and secreted with lipoproteins in patients with nonalcoholic fatty liver disease. J Clin Invest 2005; 115: 1343– 1351.

Figure captions

Fig. 1 The consumption of an MCD diet induces NASH in C57BL/6 mice

(A) Liver sections stained with hematoxylin and eosin (H&E) or Sirius red. Upper panel: control mice; lower panel: MCD mice (original magnification, ×200). Arrowheads indicate the infiltrated inflammatory cells. (B) Serum AST activity in normal and MCD mice. (n = 5 per group) (C) Serum BA concentrations in normal and MCD mice, measured by ELISA. (n = 5 per group) Values are means and SD. $^{**}p<0.01$

MCD, methionine and choline-deficient; NASH, non-alcoholic steatohepatitis; AST, aspartate transaminase; BA, bile acid; ELISA, Enzyme-Linked Immunosorbent Assay.

Fig. 2 Consumption of an MCD diet increases the expression of proinflammatory cytokines and TGF-β

(A) TNF-α, IL-6, and TGF-β mRNA expression in the liver of control and NASH mice, measured using real-time PCR (n = 5 per group), and normalized to the expression of glyceraldehyde-3-phosphate dehydrogenase (GAPDH) mRNA. (B) TNF-α and IL-6 mRNA expression in the mesenteric lymph nodes of control and MCD mice, measured using real-time PCR (n = 5 per group). Values are means and SD. $^{*}p<0.05$, $^{**}p<0.01$

MCD, methionine and choline-deficient; NASH, non-alcoholic steatohepatitis; TNF-α, tumor necrosis factor-α; IL-6, interleukin-6; TGF-β, transforming growth factor-β.

Fig. 3 Consumption of an MCD diet increases the expression of claudin-1 in the ileum

(A) *Cldn1* mRNA expression in the ileum was measured using real-time PCR (n = 5 per group) and normalized to the expression of *Gapdh* mRNA. Values are means and SD. *p<0.05. (B) Claudin-1 protein expression in the ileum, measured by western blot analysis. β-actin was used as a loading control. Densitometric analysis of claudin-1 protein expression shown. One experiment of 5 with similar results. **p<0.01 (C) Immunohistochemical staining for claudin-1 in sections of the ileum (original magnification, ×200) Arrowheads indicate expressions of claudin-1.

MCD, methionine and choline-deficient.

Fig. 4 Effects of an MCD diet and elobixibat administration on liver histology and serum and fecal BA concentrations

Mice were fed a standard or an MCD diet for 8 weeks, and half of the latter were administered 1.2 mg/kg elobixibat for the final 4 weeks, 5 days per week, by oral gavage. n= 5 per group. (A) Liver histology. Liver sections were stained using hematoxylin and eosin (H&E) or Sirius red. Upper panel: MCD mice; lower panel: MCD mice administered elobixibat (original magnification, ×200). Arrowheads indicate the infiltrated inflammatory cells. (B) Steatosis, inflammation, and fibrosis in the liver in standard diet-fed, MCD diet-fed, and MCD diet-fed and elobixibat-administered mice (n = 5 per group). (C), Serum BA concentration in each group (n = 5 per group). (D) Fecal BA

concentration in each group (n = 5 per group). Values are means and SD. **p<0.01. n.s.: non-significant.

MCD, methionine and choline-deficient; BA, bile acid.

Fig. 5 Elobixibat ameliorates the effects of an MCD diet on the expression of proinflammatory and profibrotic genes in the liver and mesenteric lymph nodes

(A) TNF-α and IL-6 mRNA expression in the liver, measured by real-time PCR (n = 5 per group). (B) TGF-β mRNA expression in the liver, measured by real-time PCR (n = 5 per group). (C) TNF-α and IL-6 mRNA expression in the MLNs, measured by real-time PCR (n = 5 per group). Values are means and SD. *p<0.05, **p<0.01

MCD, methionine and choline-deficient; TNF-α, tumor necrosis factor-α; IL-6, interleukin-6; TGF-β, transforming growth factor-β; MLN, mesenteric lymph node.

Fig. 6 Elobixibat reduces the expression of claudin-1 in the ileum

(A) *Cldn1* mRNA expression in the ileum, measured by real-time PCR (n = 5 per group). Values are means and SD. *p<0.05, **p<0.01. (B) Claudin-1 expression in the ileum, measured by western blot analysis. β-actin was used as a loading control. Densitometric analysis of claudin-1 protein expression shown. One experiment of 5 with similar results. **p<0.01 (C) Immunohistochemical staining for claudin-1 in ileal sections (original magnification, ×200). Arrows indicate expressions of

claudin-1. (D) The composition of the intestinal microbiota in standard diet-fed, MCD diet-fed, and MCD diet-fed and elobixibat-administered mice, assessed by 16S ribosomal RNA gene sequencing (n = 3 per group)

MCD, methionine and choline-deficient.

Supplemental Figure

Fig. 1 Consumption of an MCD diet and additional administration of Elobixibat doesn't change the expression of claudin-3 in the ileum

(A)*Cldn3* mRNA expression in the ileum was measured using real-time PCR (n = 5 per group) and normalized to the expression of Gapdh mRNA. Values are means and SD. (B) Claudin-3 protein expression in the ileum, measured by western blot analysis. β-actin was used as a loading control. Densitometric analysis of claudin-3 protein expression shown. One experiment of 5 with similar results.

MCD, methionine and choline-deficient.

Figure 1

A

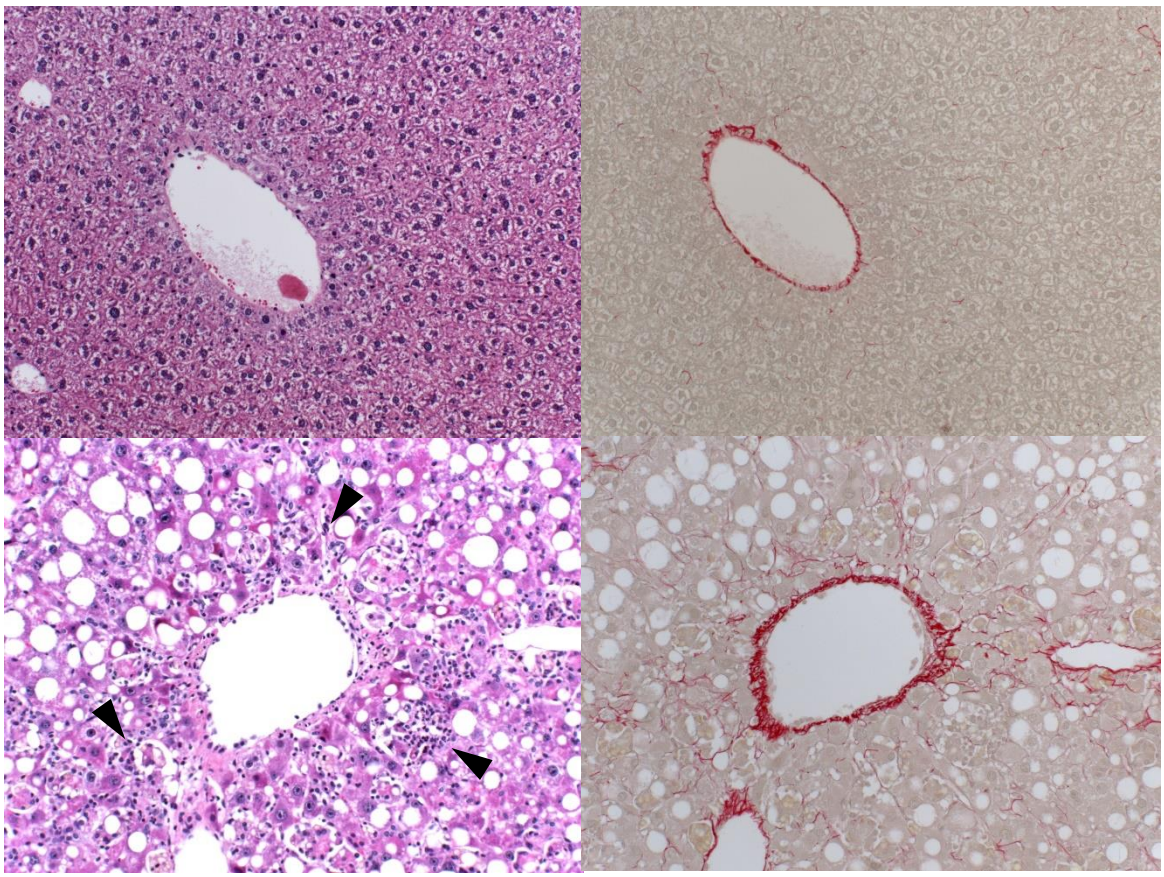

B

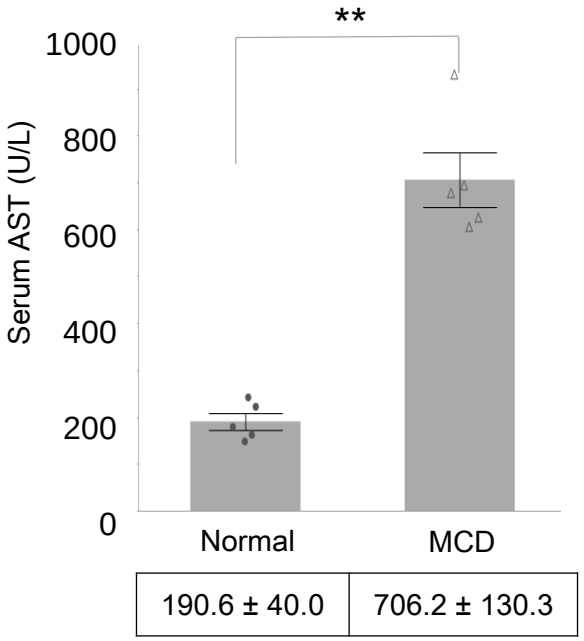

Normal	MCD
190.6 ± 40.0	706.2 ± 130.3

C

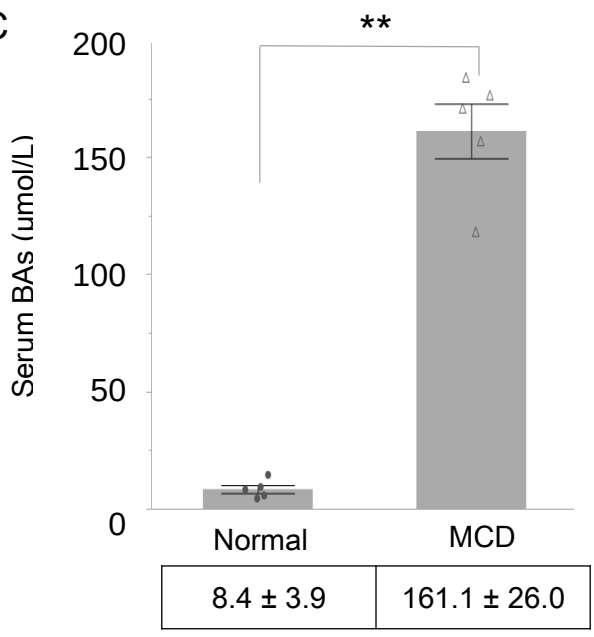

Normal	MCD
8.4 ± 3.9	161.1 ± 26.0

Figure 2

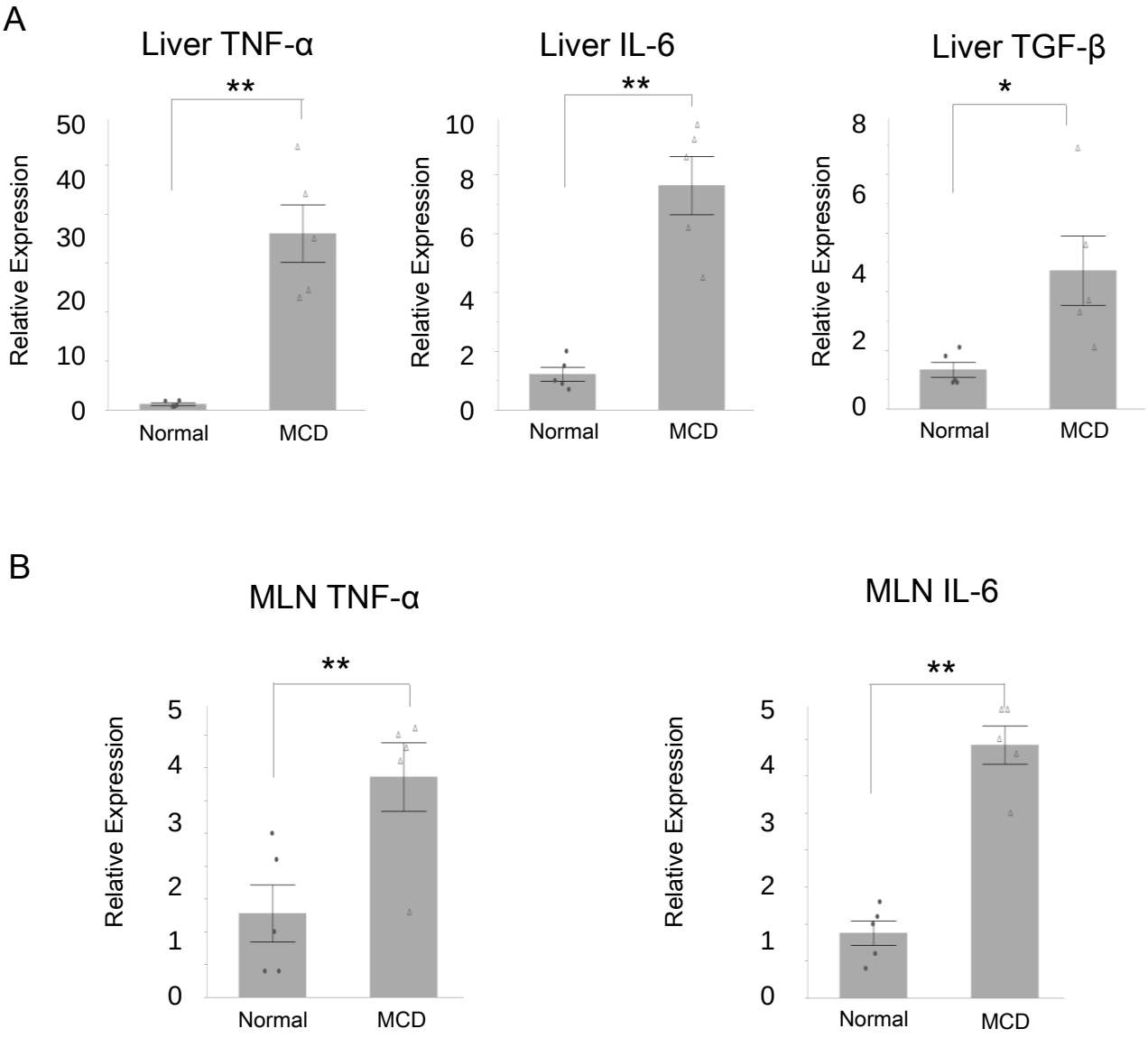
A
Liver TNF-α
**
Relative Expression
50
40
30
20
10
0
Normal
MCD
Liver IL-6
**
Relative Expression
10
8
6
4
2
0
Normal
MCD
Liver TGF-β
*
Relative Expression
8
6
4
2
0
Normal
MCD
B
MLN TNF-α
**
Relative Expression
5
4
3
2
1
0
Normal
MCD
MLN IL-6
**
Relative Expression
5
4
3
2
1
0
Normal
MCD

Figure 3

A

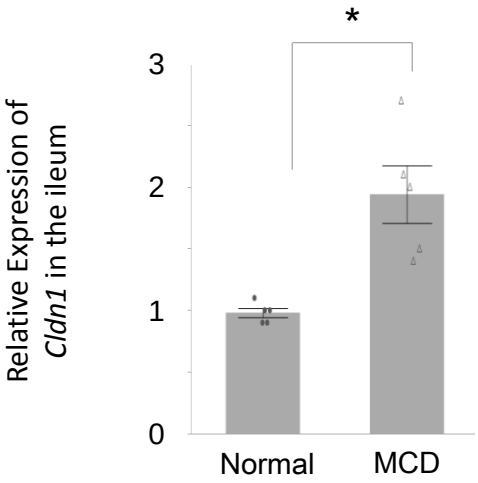

B

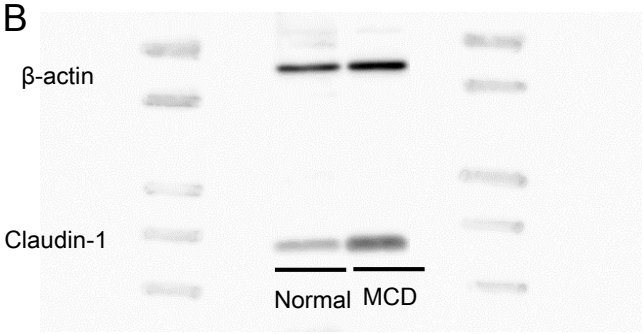

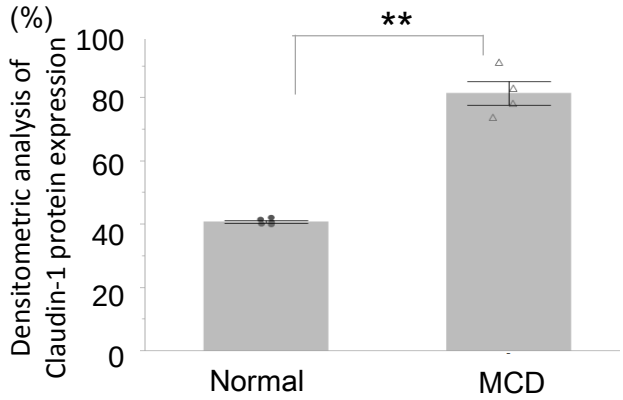

Normal	MCD
40.7 ± 0.94	81.4 ± 7.5

C

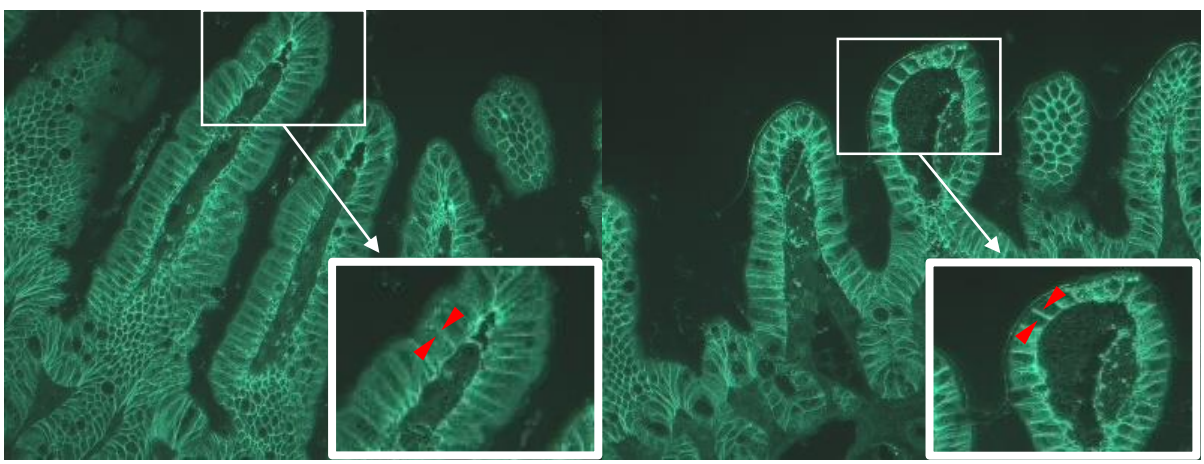

Figure 4

A

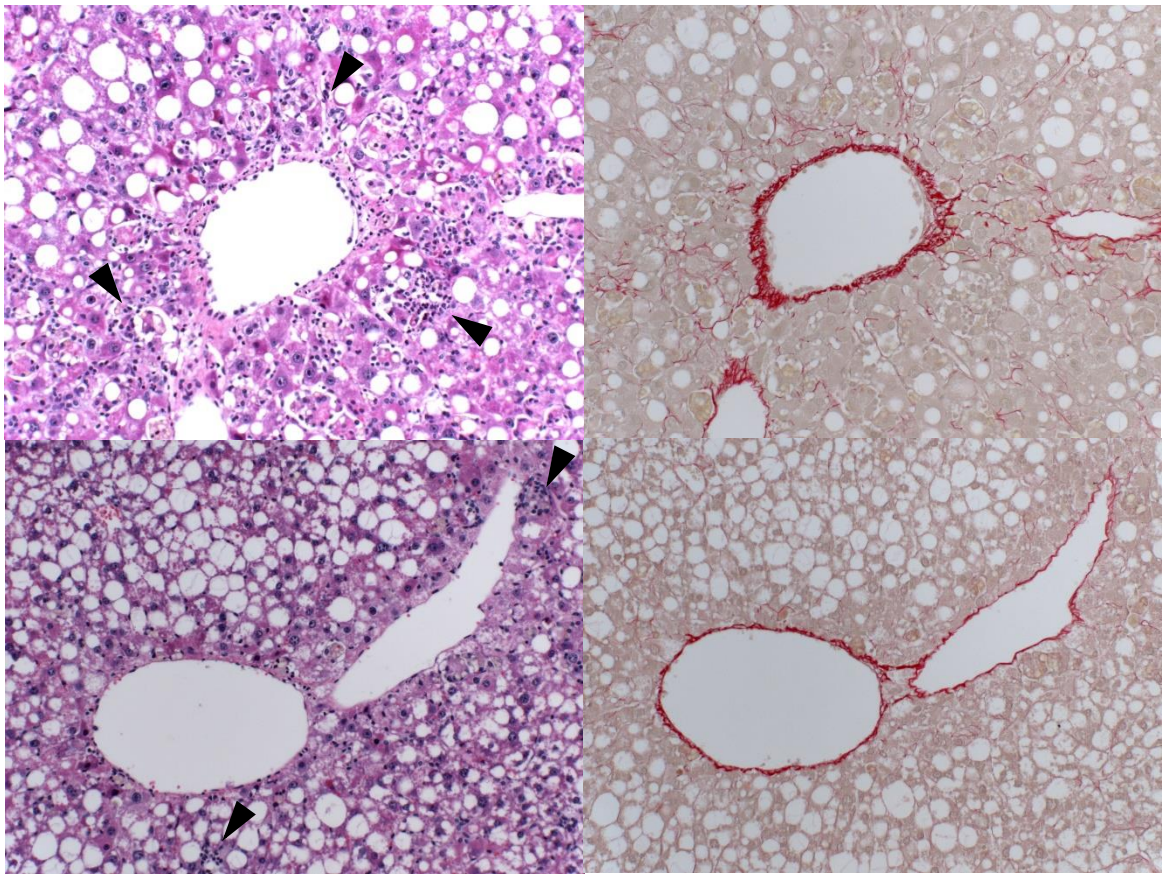

B

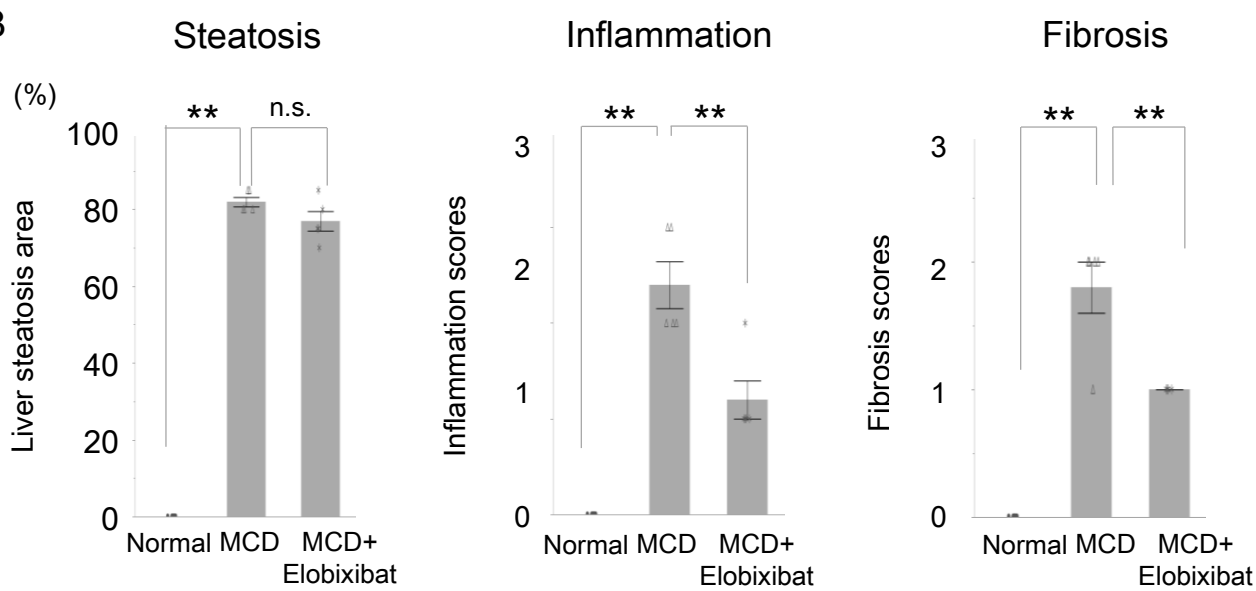

0.0 ± 0.0	82.0 ± 2.7	77.0 ± 5.7

0.0 ± 0.0	2.4 ± 0.55	1.2 ± 0.45

0.0 ± 0.0	1.8 ± 0.45	1.0 ± 0.0

Figure 4

C

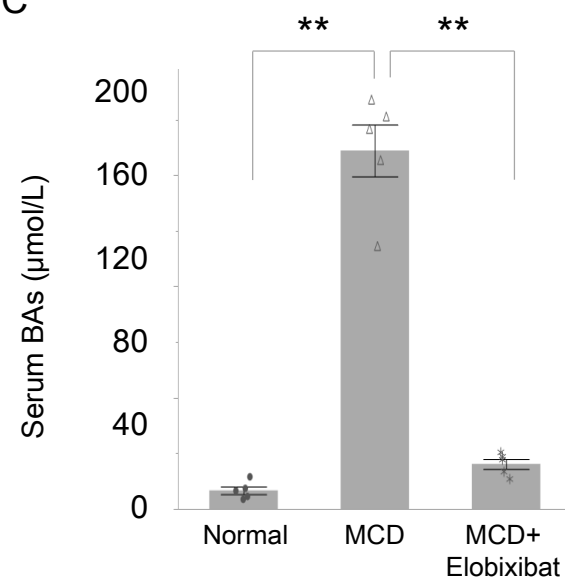

8.4 ± 3.9	161.1 ± 26.0	20.3 ± 5.0

D

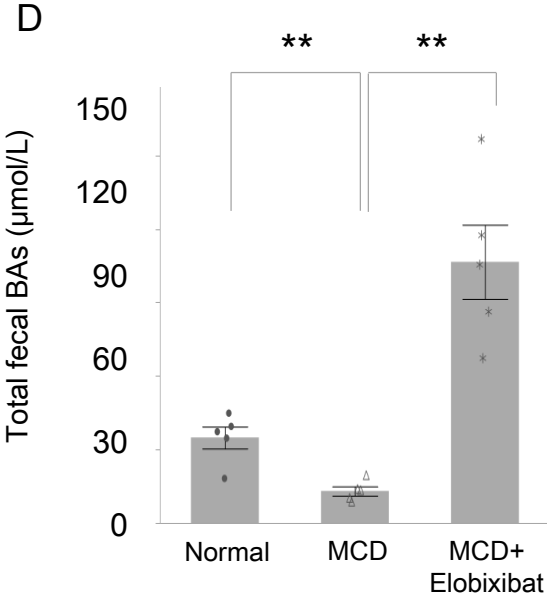

29.1 ± 8.4	10.9 ± 3.5	88.9 ± 28.2

Figure 5

A

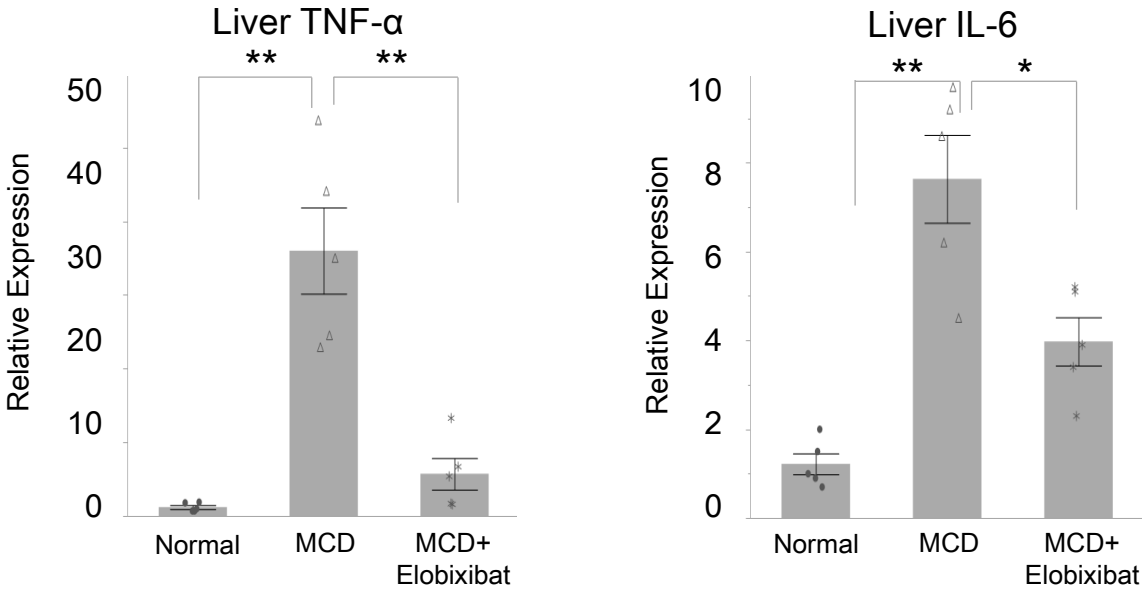
Liver TNF-α
Relative Expression
50
40
30
20
10
0
**
**
Normal
MCD
MCD+ Elobixibat
Liver IL-6
Relative Expression
10
8
6
4
2
0
**
*
Normal
MCD
MCD+ Elobixibat

B

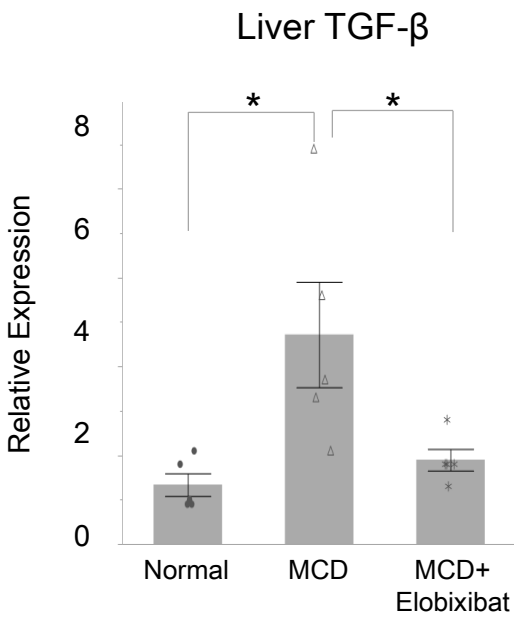
Liver TGF-β
Relative Expression
8
6
4
2
0
*
*
Normal
MCD
MCD+ Elobixibat

C

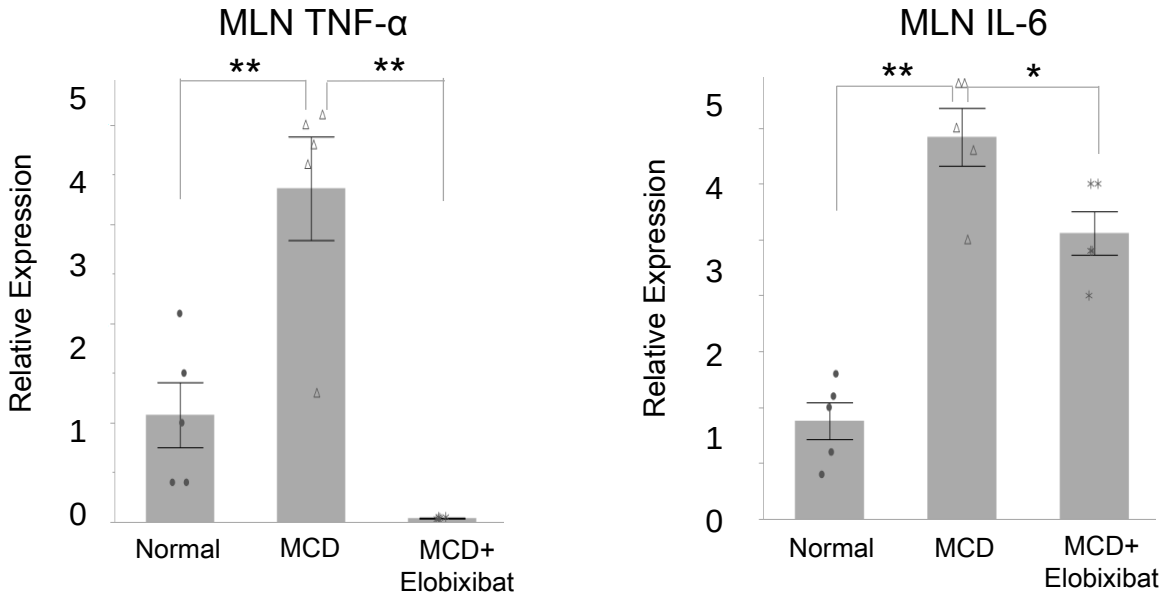
MLN TNF-α
Relative Expression
5
4
3
2
1
0
**
**
Normal
MCD
MCD+ Elobixibat
MLN IL-6
Relative Expression
5
4
3
2
1
0
**
*
Normal
MCD
MCD+ Elobixibat

Figure 6

A

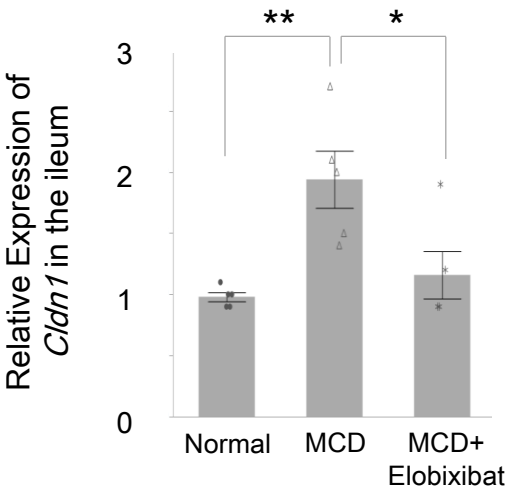

B

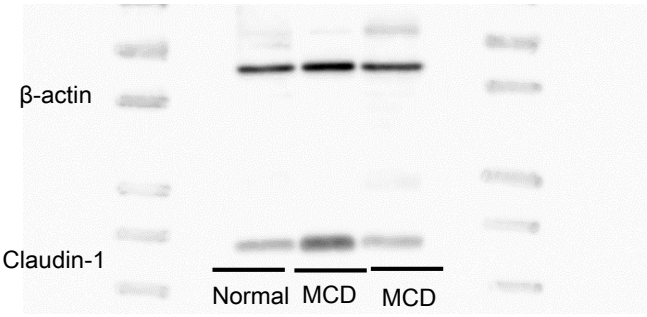

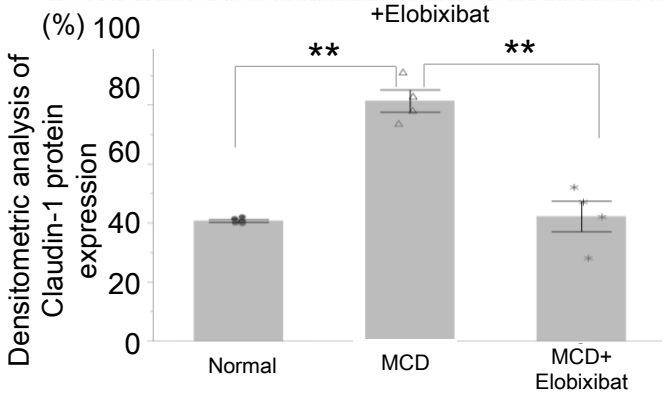

40.7 ± 0.94	81.4 ± 7.5	40.0 ± 10.3

C

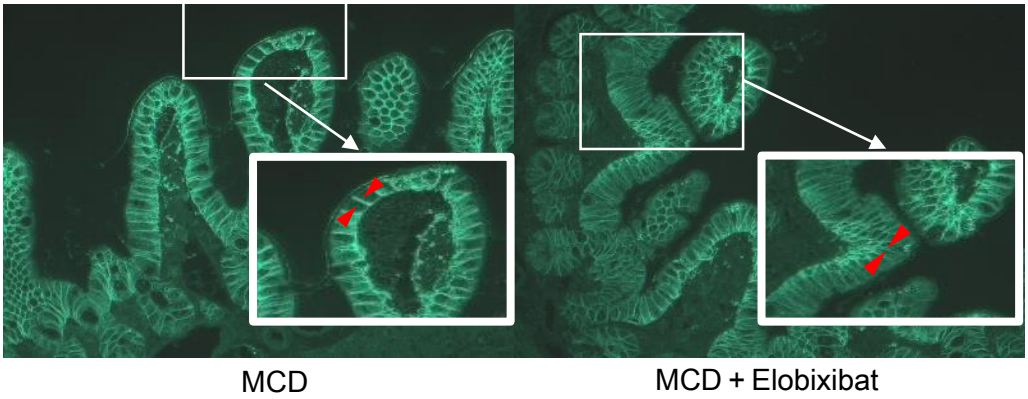

D

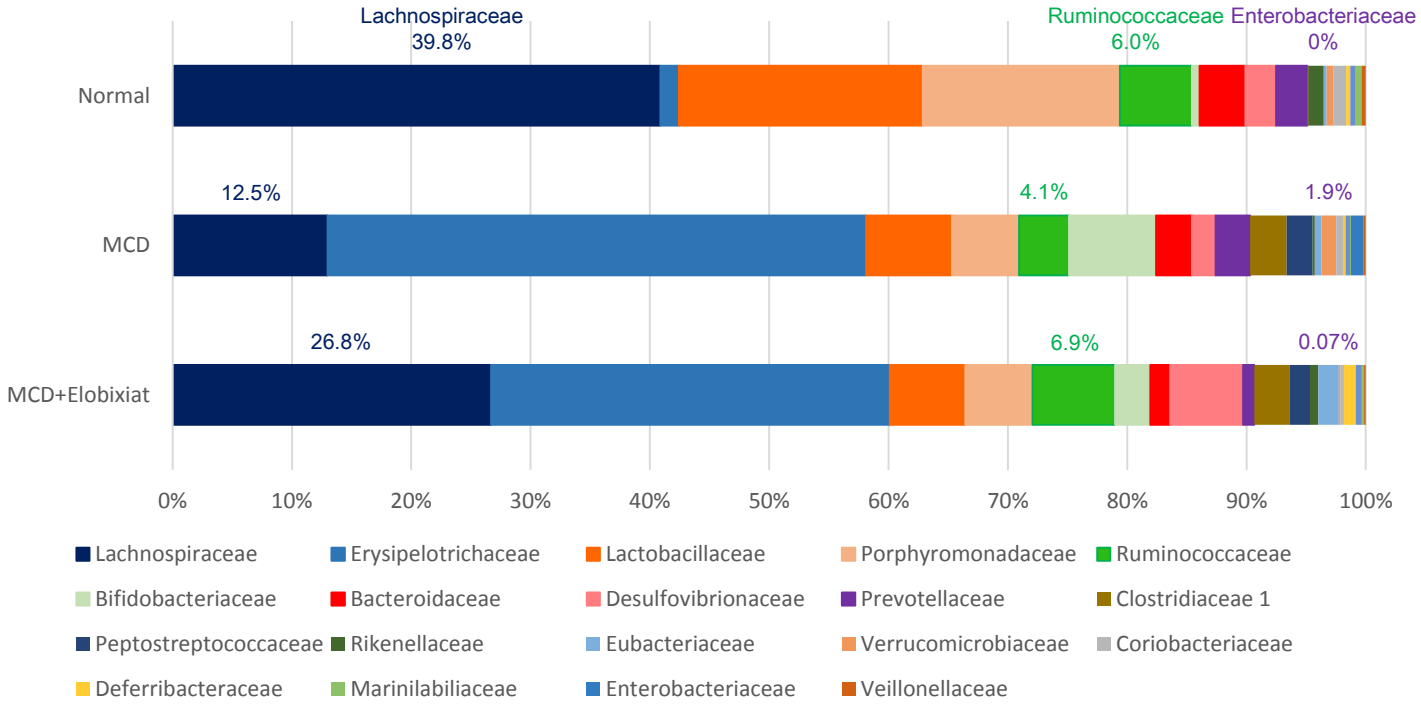

Supplemental Figure

Figure 1

A

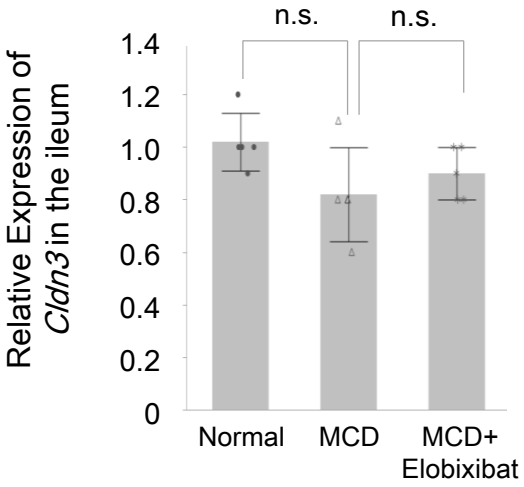

B

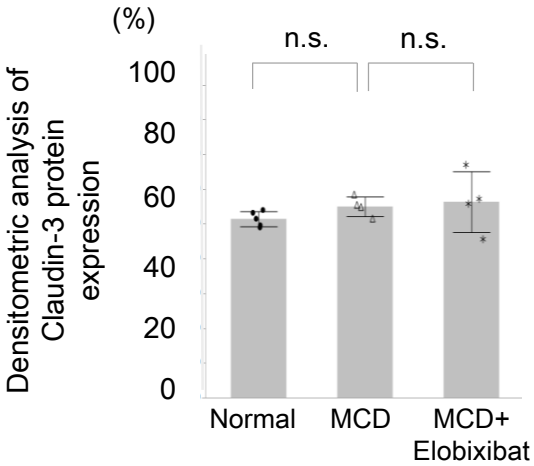

51.5 ± 2.2	55.0 ± 2.8	55.4 ± 8.7